


Information measures of quantum tunneling

A. M. Zheltikov

*Institute of Quantum Science and Engineering, Department of Physics and Astronomy,
Texas A&M University, College Station, Texas 77843, USA*

 (Received 28 December 2022; revised 30 May 2023; accepted 11 July 2023; published 1 August 2023)

A wave packet localized within a binding potential feeds an outgoing probability current as it tunnels through a finite-width potential barrier, imprinting its localization-related information on the outgoing probability-current waveform. The product of the wave number and the gradient of the outgoing probability current provides a readout for this information, connecting to the wave-packet localization, Fisher information, and related information entropy production, thus revealing the information-flow underpinning of tunneling dynamics.

DOI: [10.1103/PhysRevA.108.022201](https://doi.org/10.1103/PhysRevA.108.022201)

I. INTRODUCTION

Quantum tunneling is a fundamental physical process whereby a quantum system can overcome a binding potential as it evolves from one state of local stability to another. Since the seminal work by Hund [1,2], Oppenheimer [3,4], Fowler and Nordheim [5,6], Gamow [7], and Gurney and Condon [8,9], which laid the foundations for the theory of this phenomenon, the realm of quantum tunneling has been constantly expanding to encompass a remarkable variety of dynamical processes in physics, chemistry, and biology [10]. Due to its extremely fast timescale and low activation energy, electron tunneling in many cases serves as a universal trigger, starting a sequence of slower physical, chemical, or biological events [11]. As one example, laser-driven electron tunneling has been shown to give rise to an ultrabroadband optical response [12,13], providing a source of high-order harmonics and attosecond field waveforms [14], as well as to enable a laser control of attosecond electron dynamics in solids [15–18], thus opening a route toward petahertz optoelectronics [19,20]. Electron tunneling in living systems is central to reduction-oxidation reactions, driving adenosine triphosphate synthesis, cellular respiration, and intracellular energy flow [21–24]. Proton tunneling, on the other hand, plays the key role in a vast variety of biological processes, ranging from trans-membrane proton transfer to enzyme catalysis and intermediate metabolite isomerization [25]. On a radically different, cosmological space-time scale, quantum tunneling is believed to be a significant factor of radiation and matter transport in black-hole settings [26].

In many of these settings, tunneling junctions play a role of transducers that transform potential energy into electric current waveforms as a part of a pertinent signal-processing function. Examples include, but are in no way limited, to the generation of extremely short electric pulses in optoelectronic circuits [15,16], directed electron transfer in proteins [22,25,27], information dynamics of black holes [28], as well as trans-membrane proton transfer as a part of bio-

logical signaling [29–31]. These remarkably diverse settings clearly demonstrate the capability of tunneling to transfer, process, and transform information, acting as units of large-scale physical, chemical, and biological information systems. Understanding information aspects of tunneling is thus the key to an in-depth analysis and design of a vast class of information systems across various fields of natural sciences.

Here, we work toward developing such understanding by examining information aspects of tunneling in a setting where a wave packet is initially localized within a binding potential, but can tunnel through a finite-width potential barrier, giving rise to an outgoing probability current. We show that as this wave packet makes its way out of the potential well, tunneling through a potential barrier, it imprints its localization-related information on the outgoing probability-current waveform. This information can be read out via the wave number k_0 and the gradient κ of the outgoing probability current. We also show that the tunneling rate can be found via the product of k_0 and κ , revealing the relation between the tunneling rate and position indeterminacy, as well as between the lifetime and localization information of the tunneling wave packet.

II. TUNNELING SETUP: POTENTIAL AND WAVE FUNCTIONS

We consider a quantum system whose wave function $\Psi(x, t)$ is initially localized within a well of a binding potential (Fig. 1),

$$V(x) = \begin{cases} \infty, & x = 0 \\ 0, & 0 < x < l, x > l_1. \\ V_0, & l \leq x \leq l_1 \end{cases} \quad (1)$$

The solution to the Schrödinger equation for such a potential is

$$\Psi(x, t) = \psi(x) \exp(-iEt/\hbar), \quad (2)$$

where

$$\psi(x) = \begin{cases} 0, & x < 0, \\ \psi_I(x) = A_1 \sin(qx), & 0 < x < l \\ \psi_{II}(x) = A_2 \exp[-\alpha(x-l)] + B_2 \exp[\alpha(x-l)], & l \leq x \leq l_1 \\ \psi_{III}(x) = A_3 \exp[iq(x-l_1)], & x > l_1 \end{cases}, \quad (3)$$

$q^2 = 2m\hbar^{-2}E$, $\alpha^2 = 2m\hbar^{-2}(V_0 - E) = q_0^2 - q^2$, and E is the energy.

The continuity of $\psi(x)$ and its spatial derivative $d\psi/dx$ at the boundaries $x = l$ and $x = l_1$ leads to a characteristic equation:

$$\chi_+/\chi_- \exp(-2\alpha a) = \eta_+/\eta_-, \quad (4)$$

where $\chi_{\pm} = 1 \pm iq/\alpha$, $\eta_{\pm} = \tan(ql) \pm q/\alpha$, and $a = l_1 - l$.

With the spectrum of wave numbers q_n found by solving Eq. (4), the energy eigenvalues are defined as $E_n = \hbar^2 q_n^2/(2m)$. We search for approximate solutions to Eq. (4) in the opaque-barrier limit, with $\exp(-\alpha a) \ll 1$, in the form

$$q_n \approx k_n - i\kappa_n. \quad (5)$$

Here, k_n are the wave numbers of the wave functions solving the Schrödinger equation for a potential profile with an infinitely wide barrier (dashed-dotted line in Fig. 1),

$$V(x) = \begin{cases} \infty, & x = 0 \\ 0, & 0 < x < l. \\ V_0, & x > l \end{cases} \quad (6)$$

With a potential as defined by Eq. (6), the continuity of $\psi(x)$ and $d\psi/dx$ dictates $A_3 = 0$, leading to a characteristic equation

$$\tan(kl) = -k/\alpha. \quad (7)$$

Plugging q_n in the form of Eq. (5) with k_n as defined by Eq. (7) into Eq. (4) and solving the resulting equation in the first order in $\exp(-\alpha a)$, we find

$$\kappa_n = D_n/(4l), \quad (8)$$

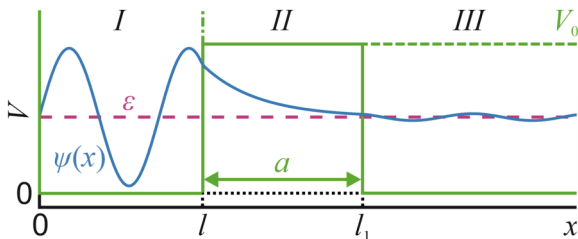


FIG. 1. Potential $V(x)$ with (solid line) a finite-depth potential well and a finite-width potential barrier, as defined by Eq. (1); (dashed line) a finite-depth potential well and an infinite-width potential barrier, as defined by Eq. (6); and (dashed-dotted line) an infinite-depth potential well. Also shown are energy ε and wave function $\psi(x) = \psi_3(x)$, as described by Eq. (3) for potential $V(x)$ with a finite-depth, finite-barrier well, $(2mV_0)^{1/2}l/\hbar = 10$, and $\alpha a = 3.2$.

where

$$D_n = \frac{16\alpha_n^2 k_n^2}{(\alpha_n^2 + k_n^2)^2} \exp(-2\alpha_n a) \quad (9)$$

and $\alpha_n^2 = 2m\hbar^{-2}V_0 - k_n^2 = q_0^2 - k_n^2$.

In this approximation, the energy eigenvalues are

$$E_n \approx \varepsilon_n - i\hbar\lambda_n/2, \quad (10)$$

with $\varepsilon_n = \hbar^2 k_n^2/(2m)$ and $\lambda_n = \hbar k_n D_n/(2ml)$. Energy eigenvalues with nonzero imaginary parts are, of course, expected as they are consistent with the generic result of the theory of quasistationary states [32].

To gain a deeper insight into the physical content of Eqs. (7)–(10), we resort to an analytical solution for the transmission of a rectangular barrier with a height V_0 and width a [33,34]:

$$D = \frac{4\alpha^2 k^2}{4\alpha^2 k^2 + q_0^4 \sinh^2(\alpha a)}. \quad (11)$$

The behavior of barrier transmission D as a function of ε/V_0 for two values of $q_0 a$ is illustrated in Fig. 2(a). For an opaque barrier, $\exp(-\alpha a) \gg 1$, Eq. (11) reduces to $D = 16\alpha^2 k^2 (\alpha^2 + k^2)^{-2} \exp(-2\alpha a)$, recovering Eq. (9) with $\alpha = \alpha_n$ and $k = k_n$.

The coefficient D_n as defined by Eq. (9) is thus recognized as the transmission of the potential barrier found in the opaque-barrier limit. With a local velocity defined as

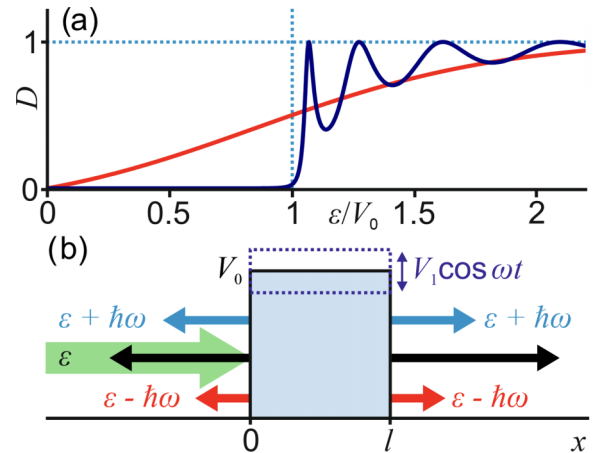


FIG. 2. (a) Barrier transmission D as a function of ε/V_0 for $(2mV_0)^{1/2}a/\hbar = 1$ (line 1) and 6 (line 2). Also shown are $\varepsilon/V_0 = 1$ line (vertical dashed line) and $D = 1$ level (horizontal dashed line). (b) Büttiker-Landauer oscillating potential barrier against an incident wave with energy ε , as well as transmitted and reflected waves with energies ε , $\varepsilon + \hbar\omega$, and $\varepsilon - \hbar\omega$.

$v_n = \hbar k_n/m$, λ_n can be expressed as

$$\lambda_n = v_n D_n / (2l), \tag{12}$$

i.e., as a product of the collision rate with a barrier $v_n/(2l)$ and the transmission of the barrier D_n . We see that λ_n can be understood as the rate at which the probability density $\rho(x, t) = |\psi(x, t)|^2$ leaks from the well via a tunneling through a finite-height, finite-width potential barrier.

III. TUNNELING QUASISTATIONARY STATES: CONTINUITY AND WAVE DYNAMICS

With the wave number q_n as defined by Eq. (7), the wave functions $\psi_n(x)$ display a weak exponential growth for $x > l_1$ with a small increment $\kappa_n \ll k_n$. Such a behavior of $\psi_n(x)$, perhaps counterintuitively, is not only consistent with, but is, in fact, dictated by the constituent equations for the probability density, such as the continuity equation.

Indeed, with a generic Madelung decomposition [35],

$$\Psi(x, t) = [\rho(x, t)]^{1/2} \exp[ims(x, t)/\hbar], \tag{13}$$

the continuity equation, $\partial\rho/\partial t + \nabla \cdot \mathbf{j} = 0$, relates the time derivative of ρ to the divergence of the probability current density $\mathbf{j} = \mathbf{v}\rho$, with $\mathbf{v} = \nabla s$ readily interpretable as the local velocity of probability-density current in the position space.

With the wave functions and energy eigenvalues as defined by Eqs. (2), (3), and (10), we find $\partial\rho_n/\partial t = -\lambda_n\rho_n$ and $j_n(x, t) = i\hbar(2m)^{-1}(\psi_n\partial\psi_n^*/\partial x - \psi_n^*\partial\psi_n/\partial x)$. Outside the potential well, i.e., for $x > l_1$, where $\rho(x, t) = A_3^2 \exp(2\kappa_n x) \exp(-\lambda_n t)$, $\nabla \cdot \mathbf{j}$ becomes $\partial j_n/\partial x = v_n \rho'_n = 2v_n \kappa_n \rho_n$. The continuity equation, $\partial\rho/\partial t + \partial j/\partial x = 0$, thus leads to

$$\lambda_n = 2\kappa_n v_n. \tag{14}$$

To appreciate the wave dynamics behind the tunneling process whereby the leakage of the probability density from the potential well feeds the outgoing probability current, we write the probability density behind the barrier as $\rho(x > l_1, t) = |\psi_{III}(x)|^2 \exp(-\lambda t) = A_3^2 \exp(2\kappa x) \exp(-\lambda t)$. Because $\lambda = 2\kappa v$ [Eq. (14)], $\rho(x > l_1, t) = A_3^2 \exp[2\kappa(x - vt)]$. Thus, for any instant of time t and any two points behind the barrier, $x_1 > l_1$ and $x_2 = x_1 + \Delta x > l_1$, we find $\rho(x_2, t)/\rho(x_1, t) = \exp(2\kappa \Delta x)$. Reaching the points x_1 and x_2 at time t are the slices of $\rho(x, t)$ that have exited the barrier at times $t_1 = t - (x_1 - l_1)/v$ and $t_2 = t - (x_2 - l_1)/v = t_1 - \Delta x/v$, respectively. For such slices, $\rho(l_1, t_2)/\rho(l_1, t_1) = \exp(-\lambda t_2)/\exp(-\lambda t_1) = \exp(\lambda \Delta x/v) = \exp(2\kappa \Delta x) = \rho(x_2, t)/\rho(x_1, t)$. We see that because the probability density at large x behind the barrier is fed by the probability density that tunnels from the well at earlier moments of time, when the probability density is higher, the $\exp(2\kappa x)$ behavior of the probability density behind the barrier is fully consistent with and directly coupled to the $\exp(-\lambda t)$ decay of the of the quasistationary state initially localized within the well, with $\lambda = 2\kappa v$.

IV. HAMILTON–JACOBI-TYPE EQUATION AND WEAK MOMENTUM

To gain further insights into the properties of wave functions defined by Eq. (3) with complex wave numbers [Eq. (5)] and complex energy eigenvalues [Eq. (10)], we observe that the phase $s(x, t)$ in the Madelung decomposition of the wave function $\Psi(x, t)$ [Eq. (13)] solves a Hamilton–Jacobi-type equation [36–38]:

$$\frac{\partial s}{\partial t} + \frac{1}{2}(\nabla s)^2 + \frac{1}{m}(V - Q) = 0, \tag{15}$$

where $Q = \hbar^2(2m)^{-1}\Delta\rho^{1/2}/\rho^{1/2}$ is the de Broglie–Bohm quantum potential [39–41].

With an osmotic velocity field defined as [37,42]

$$\mathbf{u}(x, t) = \hbar(2m)^{-1}\nabla[\ln \rho(x, t)], \tag{16}$$

the quantum potential can be expressed as $Q = mu^2/2 + (\hbar/2)\nabla \cdot \mathbf{u}$. Combining in a one-dimensional setting, $u = \hbar(2m)^{-1}\nabla(\ln \rho) = \hbar(2m)^{-1}\rho'/\rho$, $\hbar^2(2m)^{-1}(\Delta\rho^{1/2})\rho^{-1/2} = \hbar^2(8m)^{-1}[2\rho''/\rho - (\rho'/\rho)^2]$, $(m/2)u^2 = \hbar^2(8m)^{-1}(\rho'/\rho)^2$, and $(\hbar/2)u' = \hbar^2(8m)^{-1}[\rho''/\rho - (\rho'/\rho)^2]$, we find $Q = mu^2/2 + (\hbar/2)u'$.

We now recognize $m\mathbf{v} = m\nabla s$ and $m\mathbf{u}$ as the real and imaginary parts of $\mathbf{p}(\mathbf{r}) = -i\hbar\nabla[\ln \psi(\mathbf{r})]$, or, in one dimension, $p(x) = -i\hbar\nabla[\ln \psi(x)] = -i\hbar\psi'(x)/\psi(x)$, $m\mathbf{v} = \text{Re}[\mathbf{p}]$, and $m\mathbf{u} = \text{Im}[\mathbf{p}]$. Rewriting $\mathbf{p}(\mathbf{r})$ as

$$\mathbf{p}(\mathbf{r}) = \langle \mathbf{r} | \hat{\mathbf{p}} | \psi \rangle / \langle \mathbf{r} | \psi \rangle, \tag{17}$$

with $\hat{\mathbf{p}} = -i\hbar\nabla$, and interpreting $\langle \mathbf{r} | \bullet \rangle$ as postselection in the coordinate eigenstate, we are led to identify $\mathbf{p}(\mathbf{r})$ with a weak measure of the momentum. The real and imaginary parts of the local momentum $\mathbf{p}(\mathbf{r})$ as defined by Eq. (17) thus suggest a connection to weak values and weak measurements [43–49].

For a potential as defined by Eq. (1), the wave function (3) leads to $Q = [\hbar^2/(2m)]\alpha^2$ and $V - Q = E$ within the barrier region, $l \leq x \leq l_1$. In the valley behind the potential barrier, $x > l_1$, with q_n as defined by Eq. (7), Eq. (15) is seen to lead to complex energy eigenvalues E_n , recovering Eqs. (10) and (14).

V. INFORMATION MEASURE OF WAVE-PACKET LOCALIZATION AND POSITION UNCERTAINTY

In search of a suitable information metric for tunneling dynamics, we resort to a notion of Fisher information [50–52] borne by the wave function $\Psi(x, t)$ and the related probability density $\rho(x, t)$:

$$F = \int \frac{1}{\rho} \left(\frac{\partial \rho}{\partial x} \right)^2 dx. \tag{18}$$

With a one-parameter family of shifted probability densities defined as $\rho_\xi(x, t) = \rho(x - \xi, t)$, F is recognized as the Fisher information that $\rho_\xi(x, t)$ bears about ξ ,

$$F_\xi = \int \frac{1}{\rho_\xi} \left(\frac{\partial \rho_\xi}{\partial \xi} \right)^2 dx = \int \frac{1}{\rho} \left(\frac{\partial \rho}{\partial x} \right)^2 dx = F. \tag{19}$$

The Cramér–Rao lower bound [53,54] on the variance $\sigma = \sigma_\xi^2 = \langle (x - \xi)^2 \rangle$, $\sigma_\xi \geq F_\xi^{-1} = 1/F$, reveals the role of F as a quantifier of spatial localization of the wave packet $\Psi(x, t)$.

It is instructive to relate F to the kinematic parameters of a quantum system by rewriting Eq. (18) in a one-dimensional case as [55,56]

$$F = \int |\psi(x)|^2 [\psi'(x)/\psi(x) + \psi^{*'}(x)/\psi^*(x)]^2 dx, \quad (20)$$

leading to

$$F = 4\hbar^{-2}(\langle p^2 \rangle - m^2 \langle v^2 \rangle), \quad (21)$$

where the primes stand for derivatives in x , the angular brackets denote quantum-mechanical expectation values, and $p = -i\hbar\partial/\partial x$ is the momentum operator, with $\langle p^2 \rangle = \hbar^2 \int \psi^{*'}(x)\psi'(x)dx$.

Because $\mathbf{j} = \mathbf{v}\rho$, zero v implies no position-space probability current, $\mathbf{j} = 0$, with the Fisher information reaching its maximum, $F_0 = 4\hbar^{-2}\langle p^2 \rangle$, connecting to the quantum Fisher information in a spatial-shift estimation setting, including optical imaging [57–60], and showing that $\psi_{\text{opt}}(x) = \psi'(x)\langle p^2 \rangle^{-1/2}$ is an optimal wave function to read out the spatial shift of a wave packet, saturating the lower bound for the position indeterminacy σ .

Generally, because $\langle v^2 \rangle \geq 0$, the position Fisher information is upper-bounded, in accordance with Eq. (18), by

$$F \leq 4\hbar^{-2}\langle p^2 \rangle = 8m\hbar^{-2}(E - \langle V \rangle). \quad (22)$$

The spatial indeterminacy is thus lower bounded by

$$\sigma \geq F^{-1} \geq (\hbar/2)^2 \langle p^2 \rangle^{-1} = \hbar^2 [8m(E - \langle V \rangle)]^{-1}. \quad (23)$$

As a useful insight from Eq. (21), the Fisher information F , in its capacity as a measure of spatial localization of a wave packet, is proportional (see also Ref. [48]) to the difference between the expectation values of a purely quantum kinetic energy, $T_q = p^2/(2m)$, and its classical counterpart, $T_{cl} = mv^2/2$. This difference, in its turn, can be traced back to the osmotic-velocity field and viewed as a manifestation of the de Broglie–Bohm quantum potential Q . Indeed, expressing the Fisher information as $F = 4m^2\hbar^{-2} \int \rho u^2 dx = 4m^2\hbar^{-2}\langle u^2 \rangle$, we see that $\langle T_q \rangle - \langle T_{cl} \rangle$ connects to the osmotic velocity via $\langle T_q \rangle - \langle T_{cl} \rangle = \hbar^2(8m)^{-1}F = m\langle u^2 \rangle/2$, leading to $\langle T_q \rangle = \langle T_{cl} \rangle + m\langle u^2 \rangle/2$. Moreover, because $m \int \rho u^2 dx = -2\langle Q \rangle$, we find

$$\langle T_q \rangle - \langle T_{cl} \rangle = -\langle Q \rangle = \hbar^2(8m)^{-1}F. \quad (24)$$

The expectation value of the quantum potential Q thus shows up as the difference between the expectation values of the purely classical and purely quantum kinetic energies.

VI. STATIONARY-STATE LOCALIZATION INFORMATION AND POSITION UNCERTAINTY

A. An infinitely deep potential well

As one meaningful reference, we consider a particle in an infinitely deep potential well, i.e., in a potential $V_\infty(x)$ such that $V_\infty(x) = 0$ for $0 < x < l$ and $V_\infty(0) = V_\infty(l) = \infty$ (dashed-dotted line in Fig. 1). Solution of the Schrödinger equation for such a potential leads to stationary-state wave functions $\psi_n(x) = (2/l)^{1/2} \sin(k_n x)$ and $\psi_n(x) = (2/l)^{1/2} \cos(k_n x)$, where $k_n = \pi n/l$, with integer n and energy eigenvalues $E_n = (\hbar k_n)^2/(2m)$. The advective velocity for

such states is zero, $v_n = 0$, indicating no position-space probability current along x , $j = v\rho = 0$. The osmotic velocity and the Fisher information, found in accordance with Eqs. (16), (18), and (19), are $u_n(x) = (\hbar k_n/m) \cot(k_n x)$ and

$$F_n = 4k_n^2 = 4(\pi n/l)^2. \quad (25)$$

B. Resolving localized wave packets

To reflect on how higher- n eigenmodes ψ_n can resolve finer spatial features of localized wave packets, we consider a localized wave packet $\Psi(x)$ with a typical spatial extension L . Expanding this wave packet in the eigenmodes $\Psi_n(x)$, $\Psi(x) = \sum_n a_n \psi_n(x)$, with expansion coefficients a_n , we see that due to their higher information capacity, higher- n terms in this expansion encode for finer spatial features. How many terms are needed in this expansion to represent the wave packet $\Psi(x)$ depends on the spatial scale L , i.e., on how much information $|\Psi(x)|^2$ bears about localization in the position space. Because $a_n = \int \Psi(x)\psi_n^*(x)dx$, the high- n cutoff in the spectrum of the expansion coefficients a_n is defined by $1/L$. In other words, eigenmodes with a higher information capacity are needed to store more position information encoded in the wave packet $\Psi(x)$.

Specifically, for a Gaussian wave packet, $\Psi(x) \propto \exp(-x^2/4L^2)$, localized within an infinitely deep potential well of width l centered at $x = 0$, we find $\Psi_n(x)$ and $a_n \propto \exp[-(\pi nL)^2/(l)^2]$ for even $\Psi_n(x)$. The high- n cutoff in the spectrum of the expansion coefficients a_n is thus $n_c \approx l/(\pi L)$, scaling as l/L with the width of the potential well l and localization scale L of the wave packet $\Psi(x)$. The Fisher information that the $n = n_c$ mode bears about position shift is $F_c = 4/L^2$. The position-shift indeterminacy σ_ξ for such a mode is thus lower bounded by $\sigma_\xi \geq 1/F_c^{1/2}L/2$.

C. A finite-depth potential well with an infinitely wide barrier

We now observe that replacing $V(l) \rightarrow \infty$ by $V(x) = V_0$ for $x > l$ transforms the potential $V_\infty(x)$ (dashed-dotted line in Fig. 1) to a potential profile as defined by Eq. (6), yielding a potential well confined by an infinitely high potential barrier at $x = 0$ and a finite-height, but infinite-width, $a \rightarrow \infty$ barrier at $x = l$ (dashed line in Fig. 1). The characteristic equation for the eigenvalues k_n of bound states in such a well are found by solving Eq. (7). For the purposes of our analysis, it is convenient to rewrite this equation (see also Refs. [61,62]) as

$$[\sin(kl)]^2 = E/V_0. \quad (26)$$

For low-energy bound states in a high- V_0 potential well (6), the solutions for k_n are close to the k_n eigenvalues for an infinitely deep potential well. Equation (26) can then be solved approximately by expanding $\sin(kl)$ as Taylor series about πn (see also Ref. [63]), leading to $k_n \approx \pi n/l_{\text{eff}}$, where $l_{\text{eff}} = l(1 + \eta^{-1})$ is the effective width of the well and $\eta = (2mV_0)^{1/2}l/\hbar$ is a measure of the strength of the potential well as defined by Eq. (6). We now recognize $q_0 = \hbar^{-1}(2mV_0)^{1/2}$, appearing in Eqs. (3), (4), (9), (11), and (12) either explicitly or via α , as the inverse of the skin-layer depth, $\delta = l/\eta = \hbar(2mV_0)^{-1/2} = 1/q_0$. The effective width of the well can be then represented as a sum, $l_{\text{eff}} = l + \delta$, of the physical width of the well, l , and the depth of the skin layer δ .

The related position-shift Fisher information, found in accordance with Eq. (18), is

$$F_n \approx 4k_n^2 \approx 4(\pi n/l_{\text{eff}})^2 = (2\pi n)^2 l^{-2}(1 + \eta^{-1})^{-2}. \quad (27)$$

It is readily seen that Eq. (27) can be obtained by replacing l with l_{eff} in Eq. (21) for the Fisher information F for the eigenmodes of an infinitely deep potential well. Comparison of these two results for the Fisher information shows that the resolving power σ_ξ of the eigenmodes of the potential well as defined by Eq. (6) is a factor of $\approx l_{\text{eff}}/l = 1 + 1/\eta = 1 + (\hbar/l)(2mV_0)^{-1/2}$ lower than the resolving power of the eigenmodes of an infinitely deep potential well. This resolution-loss factor can be written as a ratio l_{eff}/l of the effective width of a potential well (6) with depth V_0 and width l to the width of an infinitely deep potential well. As $V_0 \rightarrow \infty$, the skin layer vanishes, $\delta \rightarrow 0$, leading to $l_{\text{eff}} \rightarrow l$. In this limit, expressions for the wave-number eigenvalues and the Fisher information recover the respective expressions for k_n and F for an infinitely deep potential well.

VII. TUNNELING-DRIVEN INFORMATION DYNAMICS

A. Information flow

As the potential profile $V(x)$ opens a valley for $x > l_1$ across a finite barrier from the potential well at $0 < x < l_1$ (solid line in Fig. 1), tunneling through this barrier ($l \leq x \leq l_1$ in Fig. 1) opens a pathway whereby the wave function can leak from the potential well to the $x > l_1$ region, where the motion is unbounded. In such a setting, purely stationary states with purely real energy eigenvalues are no longer possible. Instead, the states that used to be stationary, $q_n = k_n$, $E_n = \varepsilon_n$, $\kappa_n = 0$, and $\lambda_n = 0$, in a potential well (6) with an infinitely wide barrier, $a \rightarrow \infty$, become quasistationary as they acquire imaginary parts of q_n and E_n , leading to finite lifetimes $\tau_n = 1/\lambda_n$.

Representing the wave functions of quasistationary states [Eq. (3)] in the $x > l_1$ region as $\psi_n = \rho_n^{1/2} \exp(is_n)$, with $\rho_n = A_3^2 \exp[2\kappa_n(x - l_1)]$ and $s_n = k_n(x - l_1)$, we find for the advective and osmotic velocities $v_n = \nabla s_n = \hbar k_n/m$ and $u_n = \hbar(2m)^{-1} \rho'_n/\rho_n = \hbar \kappa_n/m$, respectively. The real and imaginary parts of the weak-value momentum for such states can be thus expressed as $\text{Re}[p_n] = \hbar k_n$ and $\text{Im}[p_n] = \hbar \kappa_n$. Equation (14) can now be rewritten as

$$\lambda_n = 2(m/\hbar)v_n u_n, \quad (28)$$

or

$$\lambda_n = 2(\text{Re}[p_n])(\text{Im}[p_n])/(m\hbar). \quad (29)$$

Using Eq. (27) to express k_n through the Fisher information F_n of the bound-state eigenfunctions $\psi_n(x)$ in a potential $V(x)$ as defined by Eq. (6), we find

$$\lambda_n \approx u_n F_n^{1/2}. \quad (30)$$

Using Eq. (8) to express u_n as $u_n = \hbar \kappa_n/m = \hbar D_n/(4ml)$, we find

$$\lambda_n = \hbar D_n F_n^{1/2}/(4ml). \quad (31)$$

The tunneling time of the wave packet, which is twice the lifetime of the probability density $\rho(x, t) = |\psi(x, t)|^2$, $\tau_n =$

$2/\lambda_n$, is thus given by

$$\tau_n \approx 2u_n^{-1} F_n^{-1/2} = 8ml F_n^{1/2} D_n^{-1}/\hbar. \quad (32)$$

B. Entropy production

The wave function $\Psi(x, t)$ that solves the Hamilton-Jacobi-Madelung equation [Eq. (15)] jointly with the continuity equation defines a Markovian diffusion process as described by the Fokker-Planck equation for $\rho(x, t) = |\psi(x, t)|^2$,

$$\frac{\partial \rho}{\partial t} + \nabla \cdot (\mathbf{b}\rho) = \frac{\hbar}{2m} \Delta \rho, \quad (33)$$

with a drift $\mathbf{b} = \mathbf{v} - \mathbf{u}$ [36–38,55,64].

Equation (16) is then recognized as Fick's first law [38,65], while the continuity equation can be expressed as Fick's second law, $\partial \rho/\partial t = -\nabla \cdot (\rho \mathbf{u}) = \hbar(2m)^{-1} \Delta \rho$. Combining Eq. (33) with Eq. (16) leads [64] to the following rate equation for the information entropy, $S = -\int \rho \ln \rho dx$:

$$\frac{dS}{dt} = \left(\frac{dS}{dt}\right)_1 - \left(\frac{dS}{dt}\right)_2, \quad (34)$$

where

$$\left(\frac{dS}{dt}\right)_1 = \frac{2m}{\hbar} \langle v^2 \rangle \quad (35)$$

is the rate at which information entropy diffuses from a quantum system, increasing the uncertainty and disorder, $(dS/dt)_1 \geq 0$, while

$$\left(\frac{dS}{dt}\right)_2 = \frac{2m}{\hbar} \langle \mathbf{b} \cdot \mathbf{v} \rangle \quad (36)$$

is the rate of information entropy change driven by external forces as dictated by a specific potential.

The total information entropy production rate is found by combining Eqs. (34)–(36), leading to

$$\frac{dS}{dt} = \frac{2m}{\hbar} \langle \mathbf{v} \cdot \mathbf{u} \rangle. \quad (37)$$

As can be seen from Eq. (37), positive correlation of the osmotic and advective velocity fields, or, equivalently, positive correlation of the real and imaginary parts of weak momentum, drives an information entropy flow, leading information entropy to change with time. This result offers important insights into Eq. (28) for the decay rate λ of the probability density $\rho(x, t)$ of a quantum system confined within a potential well with a finite-width barrier [Eq. (1)]. Derived by solving the pertinent Schrödinger equation with suitable boundary conditions, Eq. (28) expresses the decay rate λ_n via a product of v_n and u_n . When put in the perspective of Eq. (37), this product structure of λ_n is understood in terms of information entropy dynamics, thus revealing the information-flow underpinning of the tunneling-driven time evolution of the probability density $\rho(x, t)$.

The Fisher information is highly relevant in this context as a key parameter that quantifies wave-packet localization in position space, connecting the growth rate of the diffusion part of the differential entropy, $(dS/dt)_1$, to the parameters of a wave packet and a potential well. Indeed, combining Eqs. (21)

and (35), we arrive at

$$\left(\frac{dS}{dt}\right)_1 = \frac{4}{\hbar} \left[E - \langle V \rangle - \frac{mF}{2} \right]. \quad (38)$$

The localization Fisher information can be thus viewed as a driver of a diffusion-type probability-density current $\mathbf{j} = \mathbf{v}\rho$, leading to a respective entropy production as prescribed by Eqs. (34)–(36). The growth rate of the Fisher information is

$$\frac{dF}{dt} = 2\langle \mathbf{v} \cdot \nabla Q \rangle = \int \mathbf{v} \cdot \mathbf{f} dx, \quad (39)$$

with $\mathbf{f} = -\nabla P = \rho \nabla Q$, suggesting a straightforward analogy [64] with power release $\mathbf{f}\mathbf{v}$ due to the work done by an external force \mathbf{f} .

VIII. LIFETIMES OF QUASISTATIONARY STATES AND TUNNELING WAVE PACKETS

For $E_n < V_0$ bound states in potential profiles that allow no advection, such as an infinite-depth potential well or a finite-depth well with an infinite-width barrier, $a \rightarrow \infty$, zero advection, $v = 0$, leads, in accordance with Eqs. (34)–(36), to zero entropy production, $dS/dt = 0$, drives no tunneling, $\lambda_n = 0$, $\mathbf{j} = 0$, and gives rise to no uncertainty dynamics, $dF/dt = 0$. Because the information entropy remains unchanged, $dS/dt = 0$, the wave-packet dynamics is fully reversible in this setting.

In physical settings where \mathbf{v} is nonzero, on the other hand, such as a finite-depth, finite-barrier potential well, e.g., a potential well defined by [Eq. (1)], wave packets with a tighter spatial localization bear a larger Fisher information F , which translates into higher osmotic-velocity field magnitudes, via $\langle u^2 \rangle = (2m)^{-2} \hbar^2 F$, giving rise to faster tunneling [Eq. (30)], feeding stronger tunneling currents $j = v\rho$, and driving a faster information entropy dynamics [Eq. (36)].

Specifically, for a wave packet $\Psi(x) = \sum_n a_n \psi_n(x)$, Eq. (28) leads to the following result for the expectation value of the tunneling rate:

$$\langle \lambda \rangle = 2(m/\hbar) \sum_n |a_n|^2 v_n u_n = 2(m/\hbar) \langle vu \rangle. \quad (40)$$

The expectation value of the tunneling rate is thus seen to equal the information entropy production rate as described by Eq. (36). We estimate the sum in Eq. (40) as $\langle \lambda \rangle \approx 2k_m u_m n_m$, where k_m and u_m are the k_n and u_n values for $n = n_m$ at which $|a_n|^2 v_n u_n$ reaches its maximum. For a Gaussian wave packet $\Psi(x) \propto \exp(-x^2/4L^2)$, $n_m \approx (2\pi)^{-1} l/L$ and $k_m \approx 1/(2L)$, leading to

$$\langle \lambda \rangle \approx (2\pi)^{-1} l u_m / L^2. \quad (41)$$

The tunneling lifetime can now be estimated as $\tau_d = 2/\langle \lambda \rangle \approx 4\pi (l u_m)^{-1} L^2 = 4\pi (L/l) \tau_D$, where $\tau_D = L/u_m$ is the time it takes for a diffusion-type process with an osmotic velocity u_m to spread across a spatial scale L . Because the localization Fisher information for $n = n_m$ is $F_m = 1/L^2$, this

estimate for τ_d can be expressed as

$$\tau_d \approx 4\pi (l u_m F_m)^{-1}. \quad (42)$$

Equation (42) relates the lifetime τ_d to the localization information F of the tunneling wave packet.

IX. WEAK-VALUE READOUT OF TUNNELING DYNAMICS

We now see that a wave packet localized within a binding potential that allows tunneling, such as a potential (1), feeds an outgoing probability current as it tunnels through a finite-width barrier. This tunneling, as analysis presented above shows, imprints the information related to a spatial localization of the wave packet on the waveform of the outgoing probability current. This information can be read out from the wave number k_0 and the gradient κ of the outgoing probability current, which connect to the real and imaginary parts of the weak-value momentum. That important aspects of tunneling dynamics can be understood in terms of weak measurements was highlighted earlier by Steinberg [66]. Recent elegant experiments by Ramos *et al.* [67] have shown that the weak-measurement theory provides an adequate description of traversal times observed for rubidium atoms tunneling through an optical potential in a Bose-Einstein condensate. In search for a measure of time that a tunneling particle spends within the barrier region, Steinberg [66] examined a rectangular barrier extending from $x = -d/2$ to $x = d/2$ and constructed a Hermitian projection operator $\Theta_B = \Theta(x + d/2) - \Theta(x - d/2)$, whose eigenvalues were 1 and 0 and whose expectation value quantified the probability density integrated over the barrier region. As one of its central findings, Ref. [66] demonstrated that the dwell time τ_B , a parameter that is intended as a quantifier of the time that a tunneling particle spends within the barrier region, can be expressed as

$$\tau_S = D\tau_T + R\tau_R, \quad (43)$$

where D and R are the transmissivity and reflectivity of the barrier, and τ_T and τ_R are the transmission and reflection times, respectively, which can be found as ratios $\tau_T = \langle \Theta_B \rangle_{ti} / J_{in}$ and $\tau_R = \langle \Theta_B \rangle_{ri} / J_{in}$ of the weak values $\langle \Theta_B \rangle_{ti} = \langle t | \Theta_B | i \rangle / \langle t | i \rangle$ and $\langle \Theta_B \rangle_{ri} = \langle r | \Theta_B | i \rangle / \langle r | i \rangle$ to the incoming probability-current density J_{in} , which, in the free-particle tunneling setting of Ref. [66], is simply $J_{in} = \hbar q/m$.

The physical content of the weak-value readout of tunneling dynamics examined in this study is distinctly different. While the tunneling setting considered in Ref. [66] involved a free-particle wave packet that tunnels through a finite-width rectangular barrier, our study deals with a quantum state $\Psi(x, t)$ [Eqs. (2) and (3)] that is localized within a potential well (Fig. 1) and tunnels from this well through a finite-width, finite-height barrier, thus acquiring a finite decay time τ_d , as quantified by Eqs. (12) and (35)–(37). It is this lifetime τ_d , rather than the dwell time τ_S , that is the main focus of our study. While the dwell time τ_S seeks to answer the question as to how much time a tunneling particle spends in the barrier region, as highlighted in the title of Ref. [66], the lifetime τ_d is intended to answer a different question, viz., “What is the half-time of a tunneling quasi-stationary state?”

Similar to the dwell time τ_S in Ref. [66], the lifetime τ_d , as the analysis presented above shows, suggests a weak-value readout. However, while τ_S connects to the weak values of Θ_B , τ_d is expressed via a product of the real and imaginary parts of the weak momentum [Eq. (17)]. Such a structure of solution for τ_d is dictated by the continuity equation, which relates the partial time derivative of $\rho(x, t)$ to $\nabla \cdot \mathbf{j}$. Because $\nabla \cdot \mathbf{j}$ is the local outward flux from the probability-current density \mathbf{j} at point \mathbf{r} , it connects to the local momentum $\mathbf{p}(\mathbf{r}) = -i\hbar\nabla[\ln \psi(\mathbf{r})]$ [Eq. (17)]. As opposed to its operator counterpart, $\hat{\mathbf{p}} = -i\hbar\nabla$, which needs to be defined on an infinite axis to ensure hermiticity, $\mathbf{p}(\mathbf{r})$ is a local function, whose real part enters into the probability-current density as a multiplier, $\mathbf{j} = \text{Re}[\mathbf{p}]\rho/m$. For an \mathbf{r} -independent $\text{Re}[\mathbf{p}]$, the local outward flux at \mathbf{r} is then given by $\nabla \cdot \mathbf{j} = 2(\text{Re}[p_n])(\text{Im}[p_n])\rho/(m\hbar)$, leading to $\tau_d = 2/\lambda$ as found from Eqs. (28)–(32).

As is readily seen from their inner-product structure of $\mathbf{p}(\mathbf{r})$ [Eq. (17)], the advective and osmotic velocities \mathbf{v} and \mathbf{u} are the real and imaginary parts of the normalized transition amplitude $m^{-1}\langle \mathbf{r}|\hat{\mathbf{p}}|\psi\rangle/\langle \mathbf{r}|\psi\rangle$. Given a system in a preselected state $|\psi\rangle$ and with position eigenkets $|\mathbf{r}\rangle$ chosen as an expansion basis (postselection), the expectation value of the momentum $\hat{\mathbf{p}}$ can be expanded as $\langle \psi|\hat{\mathbf{p}}|\psi\rangle = \int a_\psi(\mathbf{r})\rho_\psi(\mathbf{r})d\mathbf{r}$, with $\rho_\psi(\mathbf{r}) = |\langle \mathbf{r}|\psi\rangle|^2$ and with weak values of $\hat{\mathbf{p}}$ serving as expansion coefficients, $a_\psi(\mathbf{r}) = \langle \mathbf{r}|\hat{\mathbf{p}}|\psi\rangle/\langle \mathbf{r}|\psi\rangle$.

X. WEAK-MEASUREMENT SETTING

To see how the real and imaginary parts of the weak momentum emerge in a measurement, we consider a measurement of one-dimensional momentum \hat{p} with a Stern-Gerlach apparatus, as described by a Stern-Gerlach interaction Hamiltonian [43] $\hat{H}_S = -g(t)Q \otimes \hat{p}$, where Q is a canonical variable of the pointer conjugate to its momentum P and $g(t)$ is a normalized function that describes the turn-on and turn-off of the interaction between the pointer Π and the quantum system Σ . Before this interaction is turned on, the system is preselected in a state $|\psi\rangle$ and the pointer state is $\Phi(Q) = (2\pi)^{-1/4}\Delta^{-1/2}\exp[-Q^2/(2\Delta)^2]$. With a postselected state of the system chosen as $|\varphi\rangle$ and with Δ adjusted in such a way that $\Delta \ll \langle \varphi|\psi\rangle/\langle \varphi|\hat{p}|\psi\rangle$, the time evolution imposed by the measurement unfolds as

$$\begin{aligned} & \langle \varphi|\exp\left(-i\int \hat{H}dt\right)|\psi\rangle \otimes \Phi(Q) \\ & \approx \langle \varphi|\psi\rangle \exp(iQ\langle \varphi|\hat{p}|\psi\rangle/\langle \varphi|\psi\rangle) \exp[-Q^2/(2\Delta)^2]. \end{aligned} \quad (44)$$

The momentum-space pointer state after the measurement is $\tilde{\Phi}(P) \propto \exp[-\Delta^2(P - \langle \varphi|\hat{p}|\psi\rangle/\langle \varphi|\psi\rangle)^2]$. With $|\varphi\rangle = |x\rangle$, the momentum of the pointer provides a readout for the advective velocity, $P_w = \text{Re}[\langle x|\hat{p}|\psi\rangle/\langle x|\psi\rangle] = \text{Re}[p] = mv$. The osmotic velocity, on the other hand, shows up as a Q -space shift of the pointer state, $\Phi(Q) \propto \exp[iQ\text{Re}[p]] \exp[-(2\Delta)^{-2}(Q + 2\Delta^2\text{Im}[p])^2]$. Because Δ is small, the uncertainty of individual P_w readouts is much larger than mv , $1/(2\Delta) \gg mv$. Individual readouts will thus give little information on mv , requiring a large number of measurements for accurate mv estimation. In return, as long as Δ is kept small so that $\Delta \ll \langle \varphi|\psi\rangle/\langle \varphi|\hat{p}|\psi\rangle$, the effect of a pointer on a quantum

system remains vanishingly small, as Eq. (44) shows, justifying the central idea behind weak measurements [43–47].

XI. LIFETIME τ_d VERSUS TUNNELING TIMES

The lifetime τ_d is not intended to answer the question as to how much time a tunneling particle spends within the barrier region. Instead, τ_d is a measure of how fast a quasistationary state localized in a potential well leaks from this well by tunneling through a finite-width, finite-height potential barrier. Despite this difference in their physical content and potential profile settings, it is instructive to compare τ_d with the most closely related real-valued tunneling times [33,34,68–74], such as the dwell time τ_S [33,34,68–74] and the Büttiker-Landauer time τ_{BL} [34,69,75].

A. The dwell time

Unlike the lifetime τ_d , defined for a particle tunneling from a potential well in a potential $V(x)$ as defined by Eq. (5), τ_S and τ_{BL} are all defined for a free-particle wave packet with a well-defined flux $J_{\text{in}} = \hbar k/m$, experiencing no potential until it encounters a finite-width, finite-height potential barrier. Specifically, the dwell time is defined, in a general form, in terms of J_{in} and the wave function $\psi(x)$ as

$$\tau_S = J_{\text{in}}^{-1} \int_B |\psi(x)|^2 dx, \quad (45)$$

where integration is over the barrier region.

First introduced by Smith [73] as a measure of time that a particle spends within a specific region of space averaged over all scattering channels, the dwell time was subsequently shown to be a useful quantifier of tunneling time [33,34,69]. In many cases, the dwell time τ_S can be expressed [33,34,69] as a sum of the weighted reflection and transmission times [Eq. (43)]. By its definition, the dwell time is thus distinctly different from the lifetime τ_d . Defined by Eq. (45) as the ratio of the probability (the number of particles) stored within the barrier to the incident flux, the dwell time, as pointed out by Büttiker [33], Hauge and Støvneng [34], Landauer and Martin [69], Winful [70], and other authors, can be understood as a measure of time that the incident flux has to be kept on to provide accumulation of particles within the barrier. While the dwell time τ_S is concerned with a buildup of particles within a barrier, τ_d is defined as the lifetime of a quasistationary state localized in a potential well, which slowly tunnels through a potential barrier. This time is not intended to quantify the buildup of particles in a barrier. It depends on the transmission of the barrier [Eqs. (8)–(10), (12), (14), (31), (32)] rather than the time of probability-density buildup within the barrier.

For a particle with an energy $\varepsilon = \hbar^2 k^2/(2m)$, tunneling through a rectangular barrier with a height V_0 and width a , the dwell time is [33,34,69,70]

$$\tau_S = \frac{m k}{\hbar \alpha} \frac{2\alpha a(\alpha^2 - k^2) + q_0^2 \sinh(2\alpha a)}{4k^2\alpha^2 + q_0^4 \sinh^2(\alpha a)}. \quad (46)$$

For an opaque rectangular barrier, Eq. (46) yields [33,34,69,70]

$$\tau_S = \frac{2mk}{\hbar\alpha q_0^2}. \quad (47)$$

B. The Büttiker-Landauer time

The Büttiker-Landauer tunneling time is defined [34,69,75] for a free particle with a plane-wave wave function and energy ε that tunnels through a time-dependent, oscillating rectangular potential barrier [Fig. 2(b)], $V(x, t) = V_0(x) + V_1(x)\cos(\omega t)$, with $V_1(x) = V_1$ within the barrier and zero otherwise. The solution to the Schrödinger equation with such a potential is

$$\begin{aligned} \psi_{\pm}(x, t; E) = & \exp(\pm\alpha x) \exp\left(-i\frac{\varepsilon}{\hbar}t\right) \\ & \times \sum_{n=-\infty}^{\infty} J_n\left(\frac{V_1}{\hbar\omega}\right) \exp(-in\omega t), \end{aligned} \quad (48)$$

where $J_n(x)$ are the Bessel functions.

In the Büttiker-Landauer treatment, the ratio $V_1/\hbar\omega$ is so small that the sum in n in Eq. (48) is dominated by the $n = 0, \pm 1$ terms. In the limit of very low ω , the barrier transmission T_+ for particles with energies $\varepsilon + \hbar\omega$ is equal to the barrier transmission T_- for particles with energies $\varepsilon - \hbar\omega$. Generally, however, $T_+ \neq T_-$, as $(T_+ - T_-)/(T_+ + T_-) \approx \tanh \omega\tau_{\text{BL}}$ [75], with

$$\tau_{\text{BL}} = ma/(\hbar\alpha). \quad (49)$$

That $T_+ \neq T_-$ implies that the tunneling times of particles with energies $E \pm \hbar\omega$ are different, with τ_{BL} as defined by Eq. (49) identified as the tunneling time [34,69,75].

C. Benchmarking τ_d against the dwell and Büttiker-Landauer times

Comparing Eqs. (45)–(49) for the dwell and Büttiker-Landauer times with Eqs. (8), (9), (12), (14), and (32) for the lifetime τ_d , we see that not only these times are expressed in a mathematically different way, but the whole physical content of τ_d is distinctly different from the physical content of τ_S and τ_{BL} . Indeed, the lifetime τ_d is the product $T_0 D^{-1}$ of the wave-packet oscillation period within the well, $T_0 = 2l/v = 2lm/(\hbar k)$ and the inverse of barrier transmission D . Notably, unlike the Büttiker-Landauer time τ_{BL} , which is proportional to the width of the barrier a [Eq. (49)], τ_d depends on the width of the well l . Because $v/(2l)$ is the rate at which a semi-classical particle representing a quasi-stationary state localized within the well knocks on the barrier each oscillation cycle, the inverse of the lifetime τ_d is readily understood as a product of $v/(2l)$ and barrier transmission D as a measure of a probability density that leaks out of the well per unit time.

The tunneling times τ_S and τ_{BL} , on the other hand, are intended to clock the time that a particle spends within the barrier. Thus, as opposed to τ_d [Eqs. (8), (9), (12), (14), and (32)], neither the within-the-well oscillation period T_0 nor the size of the well l enters into τ_S or τ_{BL} [Eqs. (45)–(49)], as neither T_0 nor l is even relevant to these times. Moreover, the effect that the barrier has on τ_d is very different from the way

the barrier effects enter into τ_S and τ_{BL} . Indeed, while τ_d is a product of T_0 and D^{-1} , the Büttiker-Landauer time is the ratio of the barrier width a to $u_b = \hbar\alpha/m$, which is sometimes viewed [76,77] as an effective speed within the barrier. The dwell time, on the other hand, relates to the barrier via the probability $\int_B |\psi(x)|^2 dx$ to find a particle in the barrier region. In the opaque-barrier limit, this leads to a $\tau_S = (k/q_0)^2 l_s/v$ tunneling-time structure [Eq. (47)], with a barrier skin-layer depth $l_b = 2/\alpha$ and a wavenumber-mismatch factor $(k/q_0)^2$.

D. Beyond the opaque-barrier limit

As the energy ε approaches V_0 , α tends to 0, $\exp(-\alpha a)$ is no longer small, and the opaque-barrier approximation breaks down. In this regime, the opaque-barrier-limit expressions for τ_S and τ_{BL} [Eqs. (47) and (49)] are no longer applicable. An attempt to extend these expressions to the $\varepsilon \rightarrow V_0$ regime leads to an unphysical divergence. A more general result of Eq. (46) is, however, still meaningful as an expression of the dwell time τ_S . Similarly, the lifetime τ_d for $\varepsilon \rightarrow V_0$ should be calculated with a barrier transmission D as defined by Eq. (11). As is readily seen from Eq. (11), the barrier transmission D continues to monotonically increase as ε grows past V_0 . Specifically, for $\varepsilon = V_0$ [dashed line at $\varepsilon/V_0 = 1$ in Fig. 2(a)], Eq. (11) gives $D = [1 + md^2\hbar^{-2}V_0/2]^{-1}$, while, for $\varepsilon > V_0$, we find

$$D = 4\tilde{\alpha}^2 k^2 [4\tilde{\alpha}^2 k^2 + q_0^4 \sin^2(\tilde{\alpha}a)]^{-1}, \quad (50)$$

with $\tilde{\alpha}^2 = k^2 - q_0^2$.

As can be seen from Eqs. (11) and (50), barrier transmission monotonically increases as ε grows near $\varepsilon \approx V_0$. Because τ_d is a product of T_0 and D^{-1} , it monotonically decreases near $\varepsilon \approx V_0$, following an increase in barrier transmission with a growth in ε . At $\varepsilon = V_0$, $D = [1 + md^2\hbar^{-2}V_0/2]^{-1} < 1$, as the barrier transmission continues to grow with ε . At $\varepsilon = V_0 + \pi^2\hbar^2/(8ma^2)$, however, $\sin(\tilde{\alpha}a) = 0$ in Eq. (50), and D reaches its maximum, $D = 1$. As ε continues to grow past this value, D displays an oscillatory behavior [Fig. 2(a)], reaching its maximum, $D = 1$, each time when ε passes $V_0 + \pi^2\hbar^2 n^2/(8ma^2)$ with integer n . These oscillations of D translate into oscillations of τ_d , becoming especially pronounced for large $q_0 a$ [cf. curves 1 and 2 in Fig. 2(a)]. A detailed analysis of such an oscillatory behavior of τ_d is beyond the scope of this study, which focuses on quasistationary states with energies well below V_0 . For such states, the approximation of an opaque barrier remains adequate, leading to a monotonic behavior of τ_d as a function of ε/V_0 [Fig. 2(a)].

XII. CONCLUSION

To summarize, a wave packet localized within a binding potential feeds an outgoing probability current as it tunnels through a finite-width potential barrier, imprinting its localization-related information on the outgoing probability-current waveform. This information can be read out via the wave number k_0 and the gradient κ of the outgoing probability current. We demonstrate that k_0 and κ connect to the real and imaginary parts of the weak-value momentum, thus suggesting a weak-value readout for tunneling dynamics and related information measures. We also show that the tunneling rate

can be found via the product of k_0 and κ , revealing the relation between the tunneling rate and position indeterminacy, as well as between the lifetime and localization information of the tunneling wave packet.

ACKNOWLEDGMENT

This research was supported in part by the Welch Foundation (Grant No. A-1801-20210327).

-
- [1] F. Hund, *Z. Phys.* **40**, 742 (1927).
 [2] F. Hund, *Z. Phys.* **43**, 805 (1927).
 [3] J. R. Oppenheimer, *Phys. Rev.* **31**, 66 (1928).
 [4] J. R. Oppenheimer, *Proc. Natl. Acad. Sci. USA* **14**, 363 (1928).
 [5] L. Nordheim, *Z. Phys.* **46**, 833 (1927).
 [6] R. H. Fowler and L. Nordheim, *Proc. R. Soc. Lond. A* **119**, 173 (1928).
 [7] G. Gamow, *Z. Phys.* **51**, 204 (1928).
 [8] R. W. Gurney and E. U. Condon, *Nature (London)* **122**, 439 (1928).
 [9] R. W. Gurney and E. U. Condon, *Phys. Rev.* **33**, 127 (1929).
 [10] A. M. Zheltikov, *Phys. Usp.* **60**, 1087 (2017).
 [11] A. M. Zheltikov, *IEEE Photonics J.* **3**, 255 (2011).
 [12] A. M. Zheltikov, *Phys. Usp.* **64**, 370 (2021).
 [13] A. V. Mitrofanov, D. A. Sidorov-Biryukov, M. M. Nazarov, A. A. Voronin, M. V. Rozhko, A. D. Shutov, S. V. Ryabchuk, E. E. Serebryannikov, A. B. Fedotov, and A. M. Zheltikov, *Optica* **7**, 15 (2020).
 [14] P. B. Corkum and F. Krausz, *Nat. Phys.* **3**, 381 (2007).
 [15] A. Schiffrin, T. Paasch-Colberg, N. Karpowicz, V. Apalkov, D. Gerster, S. Mühlbrandt, M. Korbman, J. Reichert, M. Schultze, S. Holzner, and J. V. Barth, *Nature (London)* **493**, 70 (2013).
 [16] M. Schultze, E. M. Bothschafter, A. Sommer, S. Holzner, W. Schweinberger, M. Fiess, M. Hofstetter, R. Kienberger, V. Apalkov, V. S. Yakovlev, and M. I. Stockman, *Nature (London)* **493**, 75 (2013).
 [17] F. Krausz and M. I. Stockman, *Nat. Photonics* **8**, 205 (2014).
 [18] A. A. Lanin, E. A. Stepanov, A. V. Mitrofanov, D. A. Sidorov-Biryukov, A. B. Fedotov, and A. M. Zheltikov, *Opt. Lett.* **44**, 1888 (2019).
 [19] A. Sommer, E. M. Bothschafter, S. A. Sato, C. Jakubeit, T. Latka, O. Razskazovskaya, H. Fattahi, M. Jobst, W. Schweinberger, V. Shirvanyan, V. S. Yakovlev, R. Kienberger, K. Yabana, N. Karpowicz, M. Schultze, and F. Krausz, *Nature (London)* **534**, 86 (2016).
 [20] M. Garg, M. Zhan, T. T. Luu, H. Lakhota, T. Klostermann, A. Guggenmos, and E. Goulielmakis, *Nature (London)* **538**, 359 (2016).
 [21] B. Chance and M. Nishimura, *Proc. Natl. Acad. Sci.* **46**, 19 (1960).
 [22] R. A. Marcus, *J. Chem. Phys.* **43**, 679 (1965).
 [23] J. J. Hopfield, *Proc. Natl. Acad. Sci.* **71**, 3640 (1974).
 [24] D. DeVault, *Q. Rev. Biophys.* **13**, 387 (1980).
 [25] C. C. Moser, J. M. Keske, K. Warncke, R. S. Farid, and P. L. Dutton, *Nature (London)* **355**, 796 (1992).
 [26] P. O. Löwdin, *Rev. Mod. Phys.* **35**, 724 (1963).
 [27] A. Kuki and P. G. Wolynes, *Science* **236**, 1647 (1987).
 [28] M. K. Parikh and F. Wilczek, *Phys. Rev. Lett.* **85**, 5042 (2000).
 [29] Y. Cha, C. J. Murray, and J. P. Klinman, *Science* **243**, 1325 (1989).
 [30] L. Masgrau, A. Roujeinikova, L. O. Johannisen, P. Hothi, J. Basran, K. E. Ranaghan, A. J. Mulholland, M. J. Sutcliffe, N. S. Scrutton, and D. Leys, *Science* **312**, 237 (2006).
 [31] R. A. Marcus, *J. Chem. Phys.* **125**, 194504 (2006).
 [32] A. I. Baz, Ya. B. Zeldovich, and A. M. Perelomov, *Scattering, Reactions, and Decays in Nonrelativistic Quantum Mechanics* (Nauka, Moscow, 1971); (Israel Program for Scientific Translations, Jerusalem, 1966).
 [33] M. Büttiker, *Phys. Rev. B* **27**, 6178 (1983).
 [34] E. H. Hauge and J. A. Støvneng, *Rev. Mod. Phys.* **61**, 917 (1989).
 [35] E. Madelung, *Z. Phys. A* **40**, 322 (1927).
 [36] I. Fényes, *Z. Phys.* **132**, 81 (1952).
 [37] E. Nelson, *Phys. Rev.* **150**, 1079 (1966).
 [38] T. Takabayashi, *Prog. Theor. Phys.* **8**, 143 (1952).
 [39] D. Bohm, *Phys. Rev.* **85**, 166 (1952).
 [40] D. Bohm and B. J. Hiley, *Phys. Rep.* **172**, 93 (1989).
 [41] P. Holland, *The Quantum Theory of Motion* (Cambridge University Press, Cambridge, 1993).
 [42] D. Bohm, B. J. Hiley, and P. N. Kaloyerou, *Phys. Rep.* **144**, 321 (1987).
 [43] Y. Aharonov, D. Z. Albert, and L. Vaidman, *Phys. Rev. Lett.* **60**, 1351 (1988).
 [44] C. R. Leavens, *Found. Phys.* **35**, 469 (2005).
 [45] O. Hosten and P. Kwiat, *Science* **319**, 787 (2008).
 [46] S. Kocsis, B. Braverman, S. Ravets, M. J. Stevens, R. P. Mirin, L. K. Shalm, and A. M. Steinberg, *Science* **332**, 1170 (2011).
 [47] A. G. Kofman, S. Ashhab, and F. Nori, *Phys. Rep.* **520**, 43 (2012).
 [48] A. S. Landsman and U. Keller, *Phys. Rep.* **547**, 1 (2015).
 [49] D. Sokolovski, *Phys. Lett. A* **380**, 1593 (2016).
 [50] R. A. Fisher, *Proc. R. Soc. Edinburgh* **42**, 321 (1922).
 [51] R. Fisher, *Proc. Camb. Philos. Soc.* **22**, 700 (1925).
 [52] R. A. Fisher, *Statistical Methods for Research Workers* (Oliver and Boyd, Edinburgh, 1925).
 [53] C. R. Rao, *Bull. Calcutta Math. Soc.* **37**, 81 (1945).
 [54] H. Cramér, *Mathematical Methods of Statistics* (Princeton University, Princeton, 1946).
 [55] P. Garbaczewski, *J. Stat. Phys.* **123**, 315 (2006).
 [56] M. J. W. Hall, *Phys. Rev. A* **62**, 012107 (2000).
 [57] R. M. Dickson, A. B. Cubitt, R. Y. Tsien, and W. E. Moerner, *Nature (London)* **388**, 355 (1997).
 [58] M. Paúr, B. Stoklasa, Z. Hradil, L. L. Sánchez-Soto, and J. Rehacek, *Optica* **3**, 1144 (2016).
 [59] M. Tsang, R. Nair, and X.-M. Lu, *Phys. Rev. X* **6**, 031033 (2016).
 [60] A. M. Zheltikov, *Opt. Lett.* **47**, 1586 (2022).
 [61] P. H. Pitkanen, *Am. J. Phys.* **23**, 111 (1955).
 [62] C. D. Cantrell, *Am. J. Phys.* **39**, 107 (1971).
 [63] B. I. Barker, G. H. Rayborn, J. W. Ioup, and G. E. Ioup, *Am. J. Phys.* **39**, 107 (1971).
 [64] P. Garbaczewski, *Entropy* **7**, 253 (2005).
 [65] E. Heifetz and E. Cohen, *Found. Phys.* **45**, 1514 (2015).
 [66] A. M. Steinberg, *Phys. Rev. Lett.* **74**, 2405 (1995).
 [67] R. Ramos, D. Spierings, I. Racicot, and A. M. Steinberg, *Nature (London)* **583**, 529 (2020).

- [68] E. P. Wigner, *Phys. Rev.* **98**, 145 (1955).
- [69] R. Landauer and T. Martin, *Rev. Mod. Phys.* **66**, 217 (1994).
- [70] H. G. Winful, *Phys. Rep.* **436**, 1 (2006).
- [71] E. E. Serebryannikov and A. M. Zheltikov, *Optica* **3**, 1201 (2016).
- [72] A. M. Zheltikov, *Phys. Rev. A* **94**, 043412 (2016).
- [73] F. T. Smith, *Phys. Rev.* **118**, 349 (1960).
- [74] D. Mugnai and A. Ranfagni, in *Time in Quantum Mechanics*, edited by J. G. Muga, R. Sala Mayato, and I. L. Egusquiza (Springer, Berlin, 2008), p. 355.
- [75] M. Büttiker and R. Landauer, *Phys. Rev. Lett.* **49**, 1739 (1982).
- [76] L. V. Keldysh, *Zh. Eksp. Teor. Fiz.* **47**, 1945 (1964) [*Sov. Phys. JETP* **20**, 1307 (1965)].
- [77] B. I. Ivlev and V. I. Mel'nikov, *Phys. Rev. Lett.* **55**, 1614 (1985).